Infrared Physics & Technology 125 (2022) 104253

Contents lists available at ScienceDirect

Infrared Physics and Technology

journal homepage: www.elsevier.com/locate/infrared

Infrared surface-plasmon-resonance attenuator for broadly controllable effective radiant temperature

R.E. Peale [a,b,*], P.N. Figueiredo [b], Justin R. Phelps [c], Kevin C. Chan [c], Reza Abdolvand [c], Evan M. Smith [d], Shivashankar Vangala [e]

[a] Physics Department, University of Central Florida, Orlando, FL 32816, United States
[b] Truventic LLC, 1209 W. Gore St., Orlando, FL 32805, United States
[c] Electrical and Computer Engineering, University of Central Florida, Orlando, FL 32816, United States
[d] KBR, Inc., Beavercreek, OH 45431, United States
[e] Air Force Research Laboratory, Sensors Directorate, Wright-Patterson Air Force Base, OH 45433, United States

ARTICLE INFO

Keywords:
Surface plasmon resonance
Infrared
Attenuator
Conducting oxide

ABSTRACT

We describe a controllable infrared plasmonic laser attenuator with application to infrared detector characterization. The device promises a broad range of effective radiant temperature and fine temperature control/resolution near ambient. The enabling mechanism is controllably-frustrated surface-plasmon-resonance using a Kretschmann prism coupler. The predicted wide dynamic range depends on optical and geometric tolerances for the coupler. To investigate these, a mid-wave-infrared coupler comprising a conducting Ga-doped ZnO film deposited directly on a right-angle sapphire prism was fabricated, tested, and compared with theory. The attenuation resonance was observed by measuring specular reflection of a p-polarized quantum cascade laser beam at 4.45 μm wavelength as a function of internal incidence angle from the coated prism face. The predicted resonance for comparison was based on ellipsometrically-obtained optical constants and film thickness. Near perfect match between theory and experiment was achieved after adjusting for experimental uncertainties in optical parameters. The results quantify the accuracy and precision with which optical constants and geometrical parameters must be known to achieve the predicted performance.

1. Introduction

Recently, an attenuator of IR laser light based on excitation of surface plasmon polaritons (SPP) was proposed [1,2]. Theoretical predictions indicate up to 9 orders of magnitude controllable variation in reflected intensity. A potential and novel application is calibration of infrared detectors over a wider range of effective radiant temperatures, and with higher speed, than can be achieved using conventional blackbodies. This paper experimentally investigates the primary infrared element to illuminate some of the challenges to realizing design predictions.

The inset of Fig. 1 schematically presents the attenuator concept. A key design element is a Kretschmann prism coupler [3] comprising an infrared-transparent prism with one face coated by a partially-transparent (optically thin) conducting film. SPPs are excited by an internally reflected beam on the conducting film. Absorption by the SPP can be frustrated by controllably bringing a metal mirror close to the film, thereby achieving controllable attenuation. The metal mirror might be pixelated to create an infrared image based on spatial intensity modulation. This paper presents an example calculation of the promising range of effective radiant temperatures that might be realized using commercially available mid-IR laser sources.

The Kretschmann coupler is also the basis of commercial Surface Plasmon Resonance (SPR) biosensors, which operate at visible and near-IR wavelengths [4]. Possible advantages of operating such sensors at mid-and long-wave IR wavelengths, and design considerations, were discussed at least as early as 2008 [5,6]. Those reports emphasized the need for novel conducting films having plasma wavelengths near the IR operating wavelength. Representative subsequent reports of Kretschmann couplers for IR SPR sensing are summarized in the discussion section.

Plasma wavelength may be defined as the value where the real part of the permittivity passes through zero and changes sign. High sensitivity for an SPR biosensor requires a sharp resonance, which means the plasma and operating wavelengths should not be too close. On the other

* Corresponding author at: Physics Department, University of Central Florida, Orlando, FL 32816, United States.
E-mail address: Robert.Peale@ucf.edu (R.E. Peale).

https://doi.org/10.1016/j.infrared.2022.104253
Received 22 September 2021; Received in revised form 13 February 2022; Accepted 7 June 2022
Available online 13 June 2022

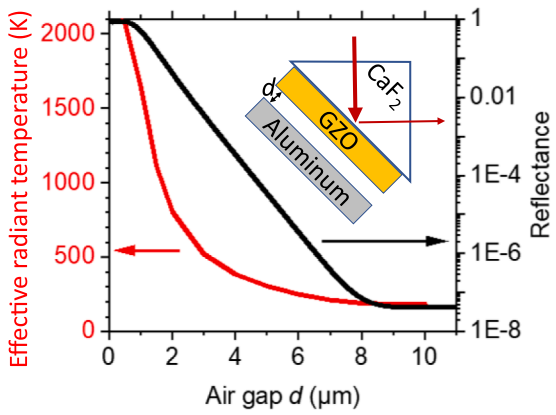

Fig. 1. Reflectance and effective radiant temperature for plasmonic prism attenuator (inset) vs. gap.

hand, good mode overlap with surface-bound biomolecules and responsivity to thin biological analytes means the plasma and operating wavelengths should not be too far separated, either.

In contrast to SPR biosensors, the controllable IR-attenuator application is better served by an angularly-broad absorption resonance [1]. This is achieved when the conducting film has plasma wavelength shorter than, but near to, the wavelength to be attenuated. To achieve the highest dynamic range requires the deepest possible absorption, for which the film thickness must be optimized. Accurate predictions require accurate high-precision values of several parameters. Uncertainties in IR optical constants and geometrical parameters affect the feasibility of realizing a theoretical design. This paper considers effects of such uncertainties.

Suitable materials with IR plasma wavelengths include conducting oxides. One such material is Ga:ZnO (Gallium-doped Zinc Oxide, or GZO) [7]. In [1], a GZO film on sapphire prism was used with a metal mirror pressed close to the GZO film to frustrate the absorption, which demonstrated the principle of controllable attenuation. However, that paper made no comparison to theoretical Fresnel-formulae predictions, which are vital to device design and optimization.

This paper compares theoretical predictions and experimental results for a GZO-coated sapphire prism as Kretschmann coupler for mid-wave IR SPPs. Use of GZO and direct coating of an IR-transparent prism with an IR SPP host to form an IR SPR coupler appear to be novel. In particular, this report investigates the effect on the calculated resonance of uncertainties in prism index, the film thickness, and its complex permittivity.

2. Theoretical methods

A Kretschmann prism coupler comprises a semi-transparent (optically thin) conducting film on one surface of a transparent dielectric prism [3]. SPPs are resonantly excited when a beam is internally incident on the film at an incidence angle beyond the critical angle for total internal reflection within the prism. The resonance angle and absorption depend on wavelength, prism index, film permittivity, and film thickness.

Excitation of SPPs by monochromatic p-polarized laser light is detected as a resonant decrease in internal specular reflectance vs incident angle. The momentum-matching condition for exciting SPPs is

$$n \sin\theta_{SPP} = Re\sqrt{\frac{\varepsilon(\omega)}{\varepsilon(\omega)+1}} \tag{1}$$

where $\varepsilon = \varepsilon' + i\,\varepsilon''$ is the complex frequency-dependent permittivity of the conductor, n the prism's refractive index, and θ_{SPP} the resonance angle of incidence within the prism. Eq. (1) resembles the condition for total internal reflection (TIR), namely $n \sin\theta_{TIR} = 1$.

On ordinary metals at IR wavelengths, ε' is negative with magnitude much larger than ε''. Hence, the SPP excitation resonance is observed at incidence angles $\theta_{SPP} > \theta_{TIR}$. However, if $|\varepsilon'|$ is very large, the angles θ_{SPP} and θ_{TIR} are almost equal, and the resonance is angularly narrow, which complicates alignment and collimation for optimum attenuation. Broad angular resonances occur when θ_{SPP} significantly exceeds θ_{TIR}, which requires the smaller negative ε' values that occur when the operating wavelength λ is just beyond the conductor's plasma wavelength λ_p.

The SPP resonance condition Eq. (1) tells nothing about the resonance strength or angular line shape. However, these are accurately calculated using Fresnel's formulae for a multi-layer system, as we have shown in [8,9]. In fact, Eq. (1) is accurate only for optically thick conducting films, which give rise to vanishingly weak and angularly narrow Kretschmann-coupler resonances. Strong resonances of convenient angular width occur with semi-transparent (optically thin) films, and such strong resonances occur at angles exceeding those predicted by Eq. (1).

The reflectance of a three-layer system is derived in [10]. The first layer is the prism material, which should be transparent, since any small loss can significantly affect the resonance. The prism's complex permittivity is $\varepsilon_1 = \varepsilon_1' + i\,\varepsilon_1''$, with ε_1'' ideally zero. The second layer is the conducting film of thickness h and complex permittivity ε_2. The third layer is air with real permittivity $\varepsilon_3 = 1$. The phase change for the beam of free-space wavelength λ in transiting the conducting film is

$$\psi = (2\pi h/\lambda)\sqrt{\left[\varepsilon_2 - \varepsilon_1 \sin^2(\theta)\right]}, \tag{2}$$

where θ is the angle of incidence within the prism. The complex wavevectors in the prism, conductor, and air are

$$k_{0z} = (2\pi/\lambda)\ \sqrt{\varepsilon_1}\ cos\theta$$

$$k_{2z} = \psi/h$$

$$k_{3z} = (2\pi/\lambda)\sqrt{\left[\varepsilon_3 - \varepsilon_1 \sin^2(\theta)\right]}, \tag{3}$$

respectively, where k_{3z} is pure imaginary for angles beyond θ_{TIR}. The complex amplitude reflection coefficients at the first and second interface, and for the whole stack, are.

$$r_{12} = (\varepsilon_2 k_{0z} - \varepsilon_1 k_{2z})/(\varepsilon_2 k_{0z} + \varepsilon_1 k_{2z})$$

$$r_{23} = (\varepsilon_3 k_{2z} - \varepsilon_2 k_{3z})/(\varepsilon_3 k_{2z} + \varepsilon_2 k_{3z})$$

$$r = (r_{12}\exp(-2i\psi) + r_{23})/(\exp(-2i\psi) + r_{12}r_{23}), \tag{4}$$

respectively. The reflectance is then $R = |r|^2$. Calculations were done in MATLAB®. In comparing to the reference reflection from a gold mirror, we consider that the beam passes through two air-sapphire interfaces, so that R should be multiplied by the square of the single surface Fresnel transmittance, ignoring multiple reflections. Over the angular range of our experiment, which is near normal incidence on the small prism faces, this baseline reflectance has the value 0.88 with an angular variation of only about 1%.

Internal incidence angle θ on the hypotenuse face of a right-angle prism (Fig. 1 inset), measured from the line through the 90 deg vertex that bisects that face, is given in terms of the external incidence angle θ_{ex} by

$$\theta = 45^{\circ} + \mathrm{Arcsin}[(1/n)\mathrm{Sin}(\theta_{ex} - 45^{\circ})] \tag{5}$$

Ellipsometry raw data does not directly give optical constants and film thicknesses. Instead, its raw data output comprises spectra for parameters ψ and Δ, which are related to the measured ratio of polarized reflectivity spectra by $R_p/R_s = \mathrm{Tan}(\psi)\ \mathrm{Exp}(i\,\Delta)$. (Note that this ψ differs from the phase change defined by Eq. (2).) If the complex permittivity

spectra and layer thicknesses are known, polarized reflectivities, and hence ψ and Δ, are accurately calculated by Fresnel's equations. However, the inverse problem is more uncertain. The approach used with the ellipsometer software is to guess the optical constants, generate ψ and Δ, compare to their measured values, and then iterate. One can generate a model for the optical constants that is accurate, and which is Kramers-Kronig consistent, but which lacks physical meaning. Alternatively, one can use a Drude model or a Sellmeier equation, for example. The results depend on the approach, so that there is unavoidable uncertainty.

To analyze the experimental ellipsometry data, a bulk sapphire model was used for the bare prism. The GZO-film permittivity was modeled using a combination of a Drude term, a Gaussian term, and a real offset, such that the permittivity is given as

$$\varepsilon(\omega) = \varepsilon_\infty - \hbar^2 / \left[\varepsilon_0 \rho \left(\tau E^2 + i\hbar E\right)\right] + Gaussian(A_n, E_n, Br) \quad (6)$$

where ε_∞, $\hbar$, ε_0, and E are the high frequency limit of the permittivity, reduced Planck's constant, free space permittivity, and light energy, respectively. The resistivity and mean scattering time are also included in the model. The Gaussian oscillator is used to model excess absorption terms using a Kramers-Kronig consistent line shape for ε'. This term includes amplitude A_n, center energy E_n, and peak broadening term Br (FWHM) as parameters to define the shape in ε". Along with these fitting parameters, the film thickness was allowed to vary to obtain the best fit, with values determined from profilometry as an initial input. The quality of the fit yielded an uncertainty estimate for the optical constants and thickness of around 1%. However, statistical and model-dependent uncertainties are significantly larger, as will be discussed.

3. Experimental details

One of the novelties of the present work is that the IR SPP host film is directly deposited on the prism coupler, as opposed to being deposited first on a substrate that is then optically coupled to the prism via an index matching fluid (see discussion section). Our integrated approach should be preferable for most applications and gives fewer layers and interfaces to consider in the analysis. Co-sputtering used Gallium Oxide and Zinc Oxide targets in an AJA sputtering system (500 W at 13.56 MHz). Depositions were first optimized using glass-wafer substrates by varying base pressure, argon and oxygen flows, rf power on each target, and prism temperature. The following brief recipe should permit reproduction by others. The deposition pressure was fixed at 2.55 mTorr. Sputtering was done in pure 20 sccm Ar flow. The rf power on the zinc oxide target was fixed at 275 Watts, the prism temperature was 275 °C. The rf power on the gallium oxide target was 75 Watts. The total deposition time was 7 min and 40 s.

A custom prism chuck facilitated the GZO deposition on the large surface of 90 deg sapphire prisms. The chuck rested on the heated platen of the sputtering system. The prism surface was heated via conduction through the chuck. To mitigate the effects of the low thermal conductivity of the sapphire, it was given a few hours to fully heat up in high vacuum before deposition. The witness slide (made of glass) was clipped to the side of the prism chuck so that the height was roughly the same as the prism surface. However, the witness slide was in poor thermal contact with the chuck. Though the temperature difference between witness and prism surfaces was likely significant, we expect that spatial location has a larger effect than temperature on thickness. Because the witness samples were off center in the sputter chamber, those films were expected to be thinner. Witness film thickness was measured at a step edge using a Dektak 150 step profilometer.

After completion of optical investigations, a destructive test was performed to obtain an independent measurement of the film thickness on the prism. We placed a drop of HCl on the GZO surface. HCl is expected to quickly attack the GZO, but it should etch the sapphire only slowly. The resulting step was then measured in the profiler.

The sheet resistance of the GZO film on the prism was measured using a 4-point probe. Optical constants for the film deposited on the prism, and for the bare prism itself, were characterized using a J.A. Woollam IR-VASE ellipsometer from 1.5 to 40 μm wavelength at several discrete incidence angles within the range 55–75 degrees in 5 or 10 degree increments.

Our use of a quantum cascade laser (QCL) to excite IR SPPs on a IR SPP host via a Kretschmann coupler is relatively novel (see discussion section) and is relevant to the application described in [2]. Measurement of specular reflectance was performed using a dual-axis goniometer with a tunable QCL (Daylight Solutions MIRcat-1400) and HgCdTe detector (Daylight Solutions HPC-2TE-100). The QCL was co-linear with a HeNe laser for alignment purposes. The reflection of the alignment laser off the front (coated) surface of the prism back onto the exit aperture of that laser defined an incidence angle of 180 degrees with an estimated angular uncertainty of ~0.3 degrees. A gold mirror was used as a reference. Resonances were measured at several wavelengths, and the conclusions of this paper apply to all those measurements. Results for one of the wavelengths are presented here for illustration.

4. Results

Fig. 1 presents calculated reflectance as a function of air–gap d between GZO surface and Al mirror for the device indicated schematically in the inset. The prism is assumed to be CaF_2 and the GZO has thickness 138.5 nm with permittivity −13.0 + i 10.8 at 5 μm wavelength. The calculation method for the four-layer system that includes the Al mirror is given in [1]. The reflected intensity is a minimum for large gaps, where it varies slowly with gap. The exponential variation is 1 decade per micron with a range of more than 7 orders.

The dynamic range of an IR detection system is often defined in terms of the temperature of a blackbody source. The effective radiant temperature of a non-blackbody source is the temperature of a blackbody having the same spectral radiance as the source [11]. Suppose that a detection system to be calibrated responds only to mid-wave IR (MWIR band, 3–5 μm wavelength). The curve of blackbody temperature vs MWIR band radiance calculated from the Planck function determines the effective radiant temperature of a spot that reflects MWIR laser light with a given radiance. If a plane wave is incident on a reflecting optic with finite dimension p, the reflected beam must diverge with solid angle $\Omega = (\lambda/p)^2$. If the incident plane wave intensity is I in units of W/m^2, the effective radiance of the reflecting optic is I/Ω, which has the usual radiance units of W/m^2-sr. For example, assume an incident laser intensity of 100 mW/cm^2 at 5 μm wavelength and a reflecting optic diameter of 40 μm. Then $\Omega = 0.016$ sr, and for the Fig. 1 reflectance limits of 4.8×10^{-8} and 0.83, the effective radiance would range from 2.7 mW/m^2-sr to 53 kW/m^2-sr, respectively. These values for the MWIR band correspond to blackbody temperatures of 190 and 2100 K, respectively. Fig. 1 presents a plot of effective radiant temperature vs. air gap for the considered example.

A promising feature demonstrated by Fig. 1 is that the change in low effective radiant temperatures with gap is very slow. Effective radiant temperature rises with decreasing gap by only 3 K/μm near $d = 10$ μm. One can control the gap to better than 100 nm using commercial piezo actuators (e.g. ThorLabs PIAK10), so that the temperature resolution can be better than 0.3 K. This is about the temperature resolution required near ambient temperature for MWIR detection and imaging systems. Finer resolution can be achieved by working at larger gaps or controlling the gap more precisely. The range of effective radiant temperatures can be shifted upward to say 300–3000 K by using higher incident IR intensity or larger mirror aperture. Such an effective radiant temperature range would cover room temperature up to the temperature of rocket exhaust [11], which would be a challenge for a most laboratory blackbody sources. Moreover, effective radiant temperature change depends on tiny movements of a mirror, so it could be altered much more rapidly than could the actual temperature of a conventional blackbody.

We next consider the challenge of fabricating a device with the predicted performance. Absolute reflectance is the critical quantity, and its minimum value should be as low as possible. These depend sensitively on optical constants and geometrical parameters. Questions include the accuracy to which the various parameters need to be known and controlled, and to what precision. The experimental results described next help to answer those questions.

The GZO film thickness on the witness sample was measured to be 150 nm, but this is expected to be smaller than the value on the prism itself. Film resistivity measured on the prism coating by the 4-point method, using the film thickness from the witness samples, was 0.6 mΩ-cm. The film thickness measured by profilometry on the step edge created by etching the prism's GZO coating was 247 nm. The step produced was not sharp, so this result is suspected to have rather large uncertainty. Any etching into the sapphire would cause this value to be an overestimate.

Ellipsometry was first performed on a surface of the bare sapphire prism to determine its optical constants. The refractive index at 4.45 μm was found to be 1.655, which agrees within 0.2% of the value 1.652 published in [12]. The extinction coefficient was determined to be 0.000. Thus, we determine the complex permittivity of the prism at 4.45 μm wavelength to be $\varepsilon_1 = 2.739 + 0$ i.

Ellipsometry was next performed on the actual GZO film deposited on the prism. The fit considered the sapphire prism to comprise a semi-infinite substrate, since any back reflections from far surfaces would not be collected by the ellipsometer. The best fit to the ellipsometry spectrum of the GZO film on the sapphire prism, using the witness sample thickness as starting value, gave a thickness of 194 ± 2 nm. If instead the larger thickness value from the destructive test was used as the starting value, the fit found a thickness of 219 nm, which is a difference of 12 %. That both ellipsometry thicknesses exceed that of the witness film is in general agreement with expectations. The permittivity spectrum of the film from the first fit is presented in Fig. 2. The zero crossing of ε' occurs at 1.50 μm wavelength. The complex permittivity at 4.45 μm wavelength is $\varepsilon_2 = -16.47 + i\,12.00$. If instead the second fit is considered, the values are 1.53 μm and $-15.09 + i\,12.69$, respectively, with the shape of the permittivity spectrum looking very similar to that in Fig. 2. The difference in the real parts of the permittivity is about 10% for these two fits. Other adequate fits are possible using different model assumptions. The effects of uncertainties in the various parameters are discussed below.

Fig. 3 presents the measured and calculated SPR curves. The agreement is nearly perfect. This mainly proves the principle that Fresnel theory must exactly predict the observed SPR resonances, if the input parameters are accurate. In fact, the agreement in Fig. 3 required a 15% decrease in the magnitude of the real part of the GZO permittivity from the Fig. 1 value and a 1% decrease in the prism index. The effects of changing the various parameters, i.e. parameter sensitivity and propagation of errors, are discussed below. These considerations are important for accurate design of plasmonic devices at IR wavelengths, where uncertainties are usually worse than at shorter wavelengths.

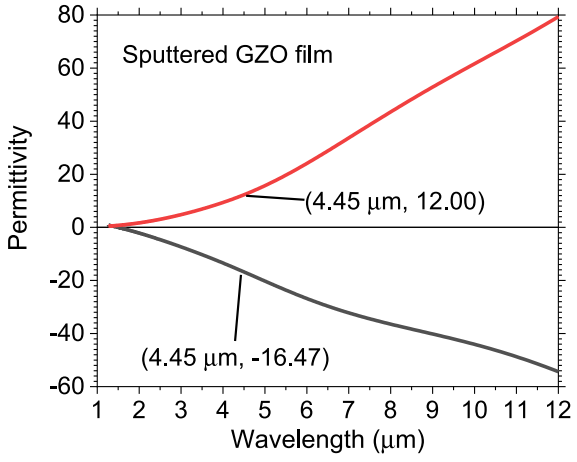

Fig. 2. Permittivity spectrum of GZO film. Values in paratheses are ε' or ε" at the given wavelength.

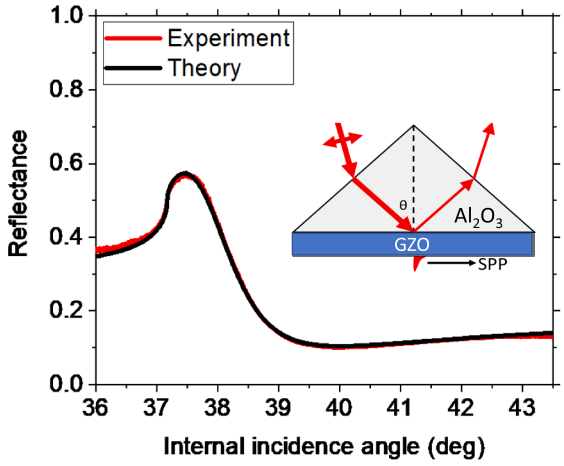

Fig. 3. Calculated and experimental reflectance for IR Kretschmann coupler (inset).

The first parameter altered was the prism index. The main effect is to shift the TIR angle, which is indicated by the nearly vertical segment on the left side of the SPR spectrum in Fig. 3. A shift in TIR by 0.39° was needed, which was achieved with a 1% decrease in prism index. This has no significant effect on any other feature of the SPR spectrum. For instance, the internal incidence angles calculated from Eq. (5) change by a comparatively insignificant 0.03°. A 1% change in the index is within our experimental uncertainty for the optical constants determined by ellipsometry. Alternatively, we can align the TIR feature by a downward shift in the experimental external incidence angles of 2%, but this exceeds our estimated experimental angle uncertainty. The calculated angular position of TIR is insensitive to the parameters of the film over their range of uncertainty.

The next parameter altered was the factor 0.88 calculated for the Fresnel reflections at entrance and exit surfaces of the prism. A scaling factor of 0.67 vertically aligns the calculation to both the measured maximum and minimum of the SPR. The unexpectedly lower measured intensities could indicate additional extinction by scattering at the GZO film and by multiple reflections within the prism, neither of which is accounted for in our calculation or present for the gold-mirror reference.

The described vertical and horizontal adjustments nearly reconciled theory and experiment, but there remained a discrepancy in the angular position of the resonance minimum by about half a degree. To decide which of the remaining parameters would be best to vary, we noted that a 10% decrease in h, $|\varepsilon'|$, or ε" produces a + 0.1, +1, or −0.5% change in the angular position of the resonance minimum. Hence, the most effective way to resolve the remaining angular discrepancy was to decrease $|\varepsilon'|$. We found that a decrease in this parameter by 15% provided agreement.

A change in h, $|\varepsilon'|$, or ε" also changes the ratio of the maximum and minimum intensity values in the calculated SPR curve. A 10% decrease in each of these increases the ratio by 39, 8, or 15%, respectively. Thus, the peak-to-valley ratio is most strongly affected by changing the film thickness. We obtained a good fit to the measured ratio, without changing either h or ε", from their values from the first ellipsometry fit. The small change to the ratio caused by the shift in ε' (previous paragraph) required a small final adjustment in the vertical scaling factor, from 0.67 to 0.69, to give the calculated curve in Fig. 3. If starting values from different ellipsometry fits were used, shifts in all three film

parameters were required, but the largest change was always to ε'.

5. Discussion and summary

The excellent agreement between experimental and calculated resonances was achieved by manually varying one parameter at a time in the order described. A better fit might have been achieved by numerical methods, but such would have been less informative regarding the effect of individual uncertainties, and the slight improvement to the fitting parameter values would have had no fundamental significance. Our approach showed that the angular position of the TIR feature on the SPR curve is almost solely governed by the prism index. The angular position of the SPR minimum is most strongly determined by the real part of the permittivity. The ratio of peak-to-valley for the SPR curve is mainly governed by the value of the film thickness, and secondly by the value of the imaginary part of the permittivity.

Optical constants determined by ellipsometry have significant uncertainties. Our SPR experiment is similar to ellipsometry, except that it produces R_p vs incidence angle at fixed wavelength rather than a spectrum of R_p/R_s at a several discrete angles. Since our SPR experiment used completely independent apparatus from ellipsometry, but the same sample, it serves as an independent check on the ellipsometric results.

This paper shows that accurate design of IR plasmonic prism couplers requires accurate knowledge of the prism index with a precision much better than 1%. Otherwise, the angular scales for theory and experiment will be off by several tenths of a degree. That is enough to cause a major difference between predicted and realized minimum reflectance at the predicted resonance angle, even for such broad resonances as considered here.

Different ellipsometry measurements gave statistical uncertainty on film thickness of order 5%, on real part of the permittivity 2%, and on imaginary part of permittivity 7%. Different models that produced reasonable fits gave differences for thickness and permittivity real- and imaginary-parts of 60, 30, and 20 %, respectively. Parameters are correlated: if thickness is increased, the magnitude of the permittivity real part must be reduced to achieve the same fit quality. The same correlation exists in fitting to the SPR spectrum, so that no matter what set of values from ellipsometry we used, we needed to reduce $|\varepsilon'|$ to a similar degree. Accurate knowledge of semiconducting film parameters to the precision required for accurate device design is a challenge because film optical properties depend strongly on deposition conditions, which may be difficult to control.

Finally, we mention some related work. There are several reports of IR SPR sensors using IR transparent prisms coated with traditional metal films [13–15]. The film may be patterned to create an effective permittivity that shifts the resonances farther into the IR [16]. Only very few studies extend deep into the mid-IR [17,18], still using conventional metals. Reference [18] used a QCL source. Conducting oxides as IR SPP hosts in fiber sensors are known [19]. Use of conducting oxides with Kretschmann couplers is relatively recent [20,21]. Pulsed-laser deposited ZnO on a sapphire substrate [20], or molecular-beam-epitaxy film of CdO on MgO substrate [21], were optically coupled to a CaF_2 prism using index-matching fluid. Agreement for the angular position of the resonance minimum between experiment and theory appears to be about 1–2 degrees, which would be inadequate for accurate design of devices such as proposed in Ref. [1].

In summary, this paper has presented predictions for an infrared plasmonic laser attenuator based on controllably-frustrated surface-plasmon-resonance using a Kretschmann coupler. A range of effective radiant temperatures that exceeds the possibilities of conventional blackbody sources was predicted. The accuracy and precision of relevant optical and geometrical parameters needed to fabricate a device with the predicted properties were considered. This comprised a comparison of calculated and experimental surface plasmon resonance at 4.45 μm wavelength for a sapphire prism coated with a conducting Ga:ZnO thin-film. Near perfect agreement between theory and experiment is achieved after reasonable adjustments for uncertainties in optical parameters. Angular differences are most strongly influenced by uncertainty in the real part of the permittivity for prism and film. Differences in resonance depth are most strongly affected by film thickness and the imaginary part of the film permittivity. Accurate prediction of absolute reflectance is important for applications such as detector calibration and that described in Ref. [2].

Declaration of Competing Interest

The authors declare the following financial interests/personal relationships which may be considered as potential competing interests: Robert E. Peale reports financial support was provided by Truventic LLC. Pedro N. Figueiredo reports financial support was provided by Truventic LLC. Robert Peale reports a relationship with Truventic LLC that includes: employment and equity or stocks. Pedro Figueiredo reports a relationship with Truventic LLC that includes: employment and equity or stocks. Pedro Figueiredo has patent #US 10,788,360, Sep. 29, 2020 issued to Truventic LLC.

Data Availability

The data that support the findings of this study are available from the corresponding author upon reasonable request.

Acknowledgments and Disclosure

Truventic and UCF authors acknowledge support from United States Air Force STTR Contract FA865118C0073 (Program Manager Dr. Joshua Lentz). EMS and SV acknowledge support from the Air Force Office of Scientific Research (Program Manager Dr. Gernot Pomrenke) under award number FA9550-19RYCOR048. This manuscript has been approved by AFRL for public release, PAIRS number 96TW-2021-0179. REP and PNF have a financial interest in Truventic, and these authors may profit from the results of this research.

References

[1] P.N. Figueiredo, S.R. DeMonaco, J.R. Phelps, R. Abdolvand, R.E. Peale, Plasmonic infrared-laser attenuator, Infrared Phys. Technol. 111 (2020) 103561, https://doi.org/10.1016/j.infrared.2020.103561.
[2] P.N. Figureiredo, Scene generation using surface plasmon polaritons, US Patent No. 10,788,360, Sep. 29, 2020.
[3] E. Kretschmann, Die Bestimmung optischer Konstanten von Metallen durch Anregung von Oberflächen-plasmaschwingungen, Z. Phys. 241 (1971) 313, https://doi.org/10.1007/BF01395428.
[4] J. Homola, S.S. Yee, G. Gauglitz, Surface Plasmon Resonance Sensors: Review, Sens. Actuators B Chem. 54 (1999) 3, https://doi.org/10.1016/S0925-4005(98)00321-9.
[5] J.W. Cleary, R.E. Peale, D. Shelton, G. Boreman, R. Soref, R.W. Buchwald, Silicides for infrared surface plasmon resonance biosensors, MRS Online Proceedings Library 1133, Article number 1003, 2008, doi.org/10.1557/PROC-1133-AA10-03.
[6] J.W. Cleary, G. Medhi, R.E. Peale, W.R. Buchwald, O. Edwards, I. Oladeji, Infrared Surface Plasmon Resonance Biosensor, Proc. SPIE 7673 (2010), 767306.
[7] R. Gibson, S. Vangala, I.O. Oladeji, E. Smith, F. Khalilzadeh-Rezaie, K. Leedy, R. E. Peale, J.W. Cleary, Conformal spray-deposited fluorine-doped tin oxide for mid- and long-wave infrared plasmonics, Opt. Mater. Express 7 (2017) 2477, https://doi.org/10.1364/OME.7.002477.
[8] R.E. Peale, E. Smith, C.W. Smith, F. Khalilzadeh-Rezaie, M. Ishigami, N. Nader, S. Vangala, J.W. Cleary, Electronic detection of surface plasmon polaritons by metal-oxide-silicon capacitor, APL Photon. 1 (6) (2016) 066103, https://doi.org/10.1063/1.4962428.
[9] P. Figueiredo, R. Peale, Plasmonic infrared attenuator, Proc. IEEE RAPID (Research and Applications of Photonics in Defense) Aug 19-21, 2019, Miramar Beach FL, paper number TuA1.3, DOI: 10.1109/RAPID.2019.8864416.
[10] L.D. Landau, E.M. Lifshitz, L.P. Pitaevskii, Electrodynamics of Continuous Media, 2nd Edition, Elsevier Butterworth Heinemann, 1984 Section 86, Problem 4.
[11] Richard D. Hudson, Jr. Infrared System Engineering, Wiley Interscience, 1969.
[12] E.D. Palik, Handbook of Optical Constants of Solids II (Academic, 1991), Chapter "Aluminum Oxide (Al_2O_3)" by F. Gervais, p. 761.
[13] R. Jha, A.K. Sharma, High-performance sensor based on surface plasmon resonance with chalcogenide prism and aluminum for detection in infrared, Optics Lett. 34 (2009) 749, https://doi.org/10.1364/OL.34.000749.

[14] R. Ziblat, V. Lirtsman, D. Davidov, B. Aroeti, Infrared Surface Plasmon Resonance: A Novel Tool for Real Time Sensing of Variations in Living Cells, Biophysical J. 90 (7) (2006) 2592–2599, https://doi.org/10.1529/biophysj.105.072090.
[15] S. Patskovsky, A.V. Kabashin, M. Meunier, J.H.T. Luong, Properties and sensing characteristics of surface-plasmon resonance in infrared light, J. Opt. Soc. Am. A 20 (2003) 1644, https://doi.org/10.1364/JOSAA.20.001644.
[16] L.L. Kegel, D. Boyne, K.S. Booksh, Sensing with prism-based near-infrared surface plasmon resonance spectroscopy on nanohole array platforms, Anal. Chem. 86 (7) (2014) 3355–3364, https://doi.org/10.1021/ac4035218.
[17] M. Golosovsky, V. Lirtsman, V. Yashunsky, D. Davidov, B. Aroeti, Midinfrared surface-plasmon resonance: A novel biophysical tool for studying living cells, J. Appl. Phys. 105 (2009), 102036, https://doi.org/10.1063/1.3116143.
[18] S. Herminjard, Mid-infrared surface plasmon resonance sensing applied to refractive index measurements of liquids (Lausanne, EPFL, 2010) doi: 10.5075/epfl-thesis-4603.
[19] J. Martínez, A. Ródenas, M. Aguiló, T. Fernandez, J. Solis, F. Díaz, Mid-infrared surface plasmon polariton chemical sensing on fiber-coupled ITO coated glass, Optics Lett. 41 (2016) 2493, https://doi.org/10.1364/OL.41.002493.
[20] E. Sachet, M.D. Losego, J. Guske, S. Franzen, J.-P. Maria, Mid-infrared surface plasmon resonance in zinc oxide semiconductor thin films, Appl. Phys. Lett. 102 (2013), 051111, https://doi.org/10.1063/1.4791700.
[21] E. Sachet, C.T. Shelton, J.S. Harris, B.E. Gaddy, D.L. Irving, S. Curtarolo, B. F. Donovan, P.E. Hopkins, P.A. Sharma, A.L. Sharma, J. Ihlefeld, S. Franzen, J.-P. Maria, Dysprosium-doped cadmium oxide as a gateway material for mid-infrared plasmonics, Nat. Mater. 14 (2015) 414, https://doi.org/10.1038/nmat4203.